# Doping Induced Evolution of Fermi Surface in Low Carrier Superconductor Tl-Doped PbTe

K. Nakayama,[1] T. Sato,[1] T. Takahashi,[1,2] and H. Murakami[3]
[1]*Department of Physics, Tohoku University, Sendai 980-8578, Japan*
[2]*WPI Research Center, Advanced Institute for Materials Research, Tohoku University, Sendai 980-8577, Japan*
[3]*Institute of Laser Engineering, Osaka University, Osaka 565-0871, Japan*
(Received 7 August 2007; published 5 June 2008)

We have performed high-resolution angle-resolved photoemission spectroscopy on Tl-doped PbTe. We observed a distinct energy shift of the valence band and core levels upon Tl doping, together with the evolution of a small hole pocket around the $\bar{X}$ point in the Brillouin zone, while no clear evidence for the localized states near the Fermi level is observed. These experimental results suggest that direct hole doping into the valence band and resultant emergence of a small Fermi surface are responsible for the metallic conductivity in Tl-doped PbTe.

DOI: 10.1103/PhysRevLett.100.227004 PACS numbers: 74.70.Dd, 71.18.+y, 74.25.Jb, 79.60.Bm

According to the Bardeen-Cooper-Shrieffer (BCS) theory, superconductivity occurs when two electrons with opposite spins condensate into a Cooper pair [1]. The BCS theory provides an excellent description of various physical properties of conventional superconductors by assuming an isotropic electron-phonon coupling. However, it is also well known that the physical properties of some other superconductors show a remarkable deviation from the conventional behavior, requesting an exotic superconducting (SC) mechanism beyond the simple electron-phonon coupling scenario. Typical examples are the spin-mediated superconductivity as discussed in high-$T_c$ cuprates and heavy fermions [2], and the charge-mediated superconductivity as suggested in organic superconductors [3].

The impurity-doped narrow-gap semiconductor Tl-doped PbTe has also drawn considerable interest since its SC properties apparently deviate from the conventional behavior [4]. For example, the carrier concentration ($\sim 10^{20}$ cm$^{-3}$) at the maximum $T_c$ ($\sim 1.5$ K for Tl concentration of $x \sim 1.5$ at.%) is 2 orders of magnitude lower than that of normal metals ($\sim 10^{22}$ cm$^{-3}$) with a similar $T_c$ value [4,5]. Superconductivity is not observed in other impurity-substituted PbTe even when the carrier concentration is similar to the Tl-doped one [6]. The $T_c$ value monotonically increases with Tl doping up to the solubility limit of $x \sim 1.5$ at.%, while the carrier concentration is almost saturated beyond a critical Tl concentration ($x_c \sim 0.3$ at.%) [6–8].

To explain these anomalous properties, two different types of theoretical models based on the localized impurity states [5,8,9] or the negative-$U$ effect [5,8,10–13] have been proposed, although the applicability of these models is highly controversial at present. In the former model, Tl doping produces localized states with a relatively large density of states (DOS) at the top of the valence band to pin the Fermi level ($E_F$) there [9]. In this case, the occurrence of superconductivity is most likely explained by the electron-phonon coupling. In the latter model, the Tl impurity itself causes the electron pairing by acting as a negative-$U$ center, and the existence of two different valences in Tl ions ($Tl^+$ and $Tl^{3+}$) is essential for stabilizing the superconductivity [10–13]. It has been suggested from the experiments of low-temperature transport properties [6,14] and the theoretical interpretation [13,15] that the valence fluctuation between $Tl^+$ and $Tl^{3+}$ ions plays a crucial role for the superconductivity (charge Kondo model). To examine the validity of these models as well as to elucidate the origin of anomalous physical properties of Tl-doped PbTe, it is essential to directly observe the change of the band structure and the Fermi surface (FS) upon Tl doping.

In this Letter, we report results of high-resolution angle-resolved photoemission spectroscopy (ARPES) on $Pb_{1-x}Tl_xTe$ ($x = 0.0$ and 0.5 at.%). We have determined the valence band as well as the near-$E_F$ band structure, and directly observed the change of the electronic structure upon Tl doping. We found that the metallic conductivity in Tl-doped PbTe arises from a small FS at $\bar{X}$ point in the surface Brillouin zone (BZ) produced by the direct hole doping into the valence band. We discuss the implication of present experimental results in comparison with theoretical models based on the impurity states [5,8,9] or the negative-$U$ effect [5,8,10–13].

High-quality single crystals of $Pb_{1-x}Tl_xTe$ were grown by the Bridgman method. We used pristine ($x = 0.0$%) and SC ($x = 0.5$ at.%, $T_c = 0.35$ K) samples for ARPES measurements. We have performed ARPES measurements using a SES2002 spectrometer with high-flux discharge lamp and a toroidal grating monochromator. We used the He I$\alpha$ and He II$\alpha$ resonance lines ($h\nu = 21.218$ and 40.814 eV, respectively) to excite photoelectrons. The energy and angular resolutions were set at 7–16 meV and 0.2°, respectively. The sample was cleaved or scraped *in situ* along the (001) plane at 20 K in a vacuum of $2 \times 10^{-11}$ Torr.

Figure 1(a) shows the bulk fcc BZ of PbTe (black lines), together with its surface BZ projected onto the (001) plane (blue rectangle). We measured valence-band ARPES spectra of pristine PbTe at 20 K along two representative cuts, $\Gamma K$ and $\Gamma X$ directions [Figs. 1(b) and 1(c), respectively], as a function of polar angle with respect to the surface normal

 

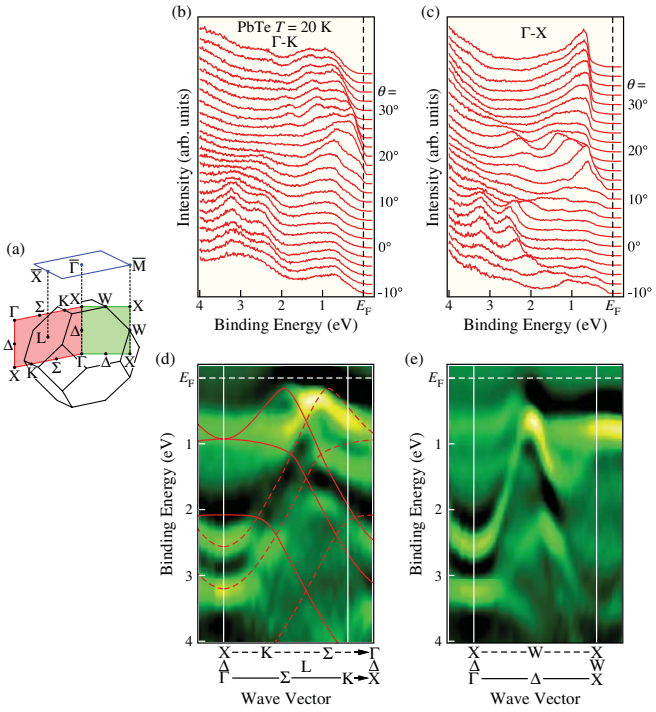


FIG. 1 (color). (a) Bulk fcc BZ of PbTe (black solid lines) and the surface BZ projected onto the (001) plane (blue rectangle). Red and green shaded areas correspond to the emission planes for the ARPES measurements along two high-symmetry lines, $\Gamma K$ and $\Gamma X$, respectively. (b) and (c) Valence-band ARPES spectra of pristine PbTe measured with He I$\alpha$ line at 20 K along the $\Gamma K$ and $\Gamma X$ directions, respectively. Polar angle ($\theta$) with respect to the surface normal is denoted. (d) and (e) Experimental band structures of PbTe along the $\Gamma K$ and $\Gamma X$ directions, respectively. Bright areas correspond to bands. Calculated bands [16] are also shown by red solid ($k_z = 0$) and broken ($k_z = \pi$) lines.

($\theta$). In the $\Gamma K$ cut [Fig. 1(b)], we find peaks at 0.9, 2.5, and 3.2 eV binding energy at $\theta = 0°$, which all show holelike dispersion centered at $\theta = 0°$. We also find another band at around 0.9 eV at $\theta = 38°$, which approaches $E_F$ with reducing $\theta$ and disperses back toward higher binding energy at $\theta < 20°$. In the $\Gamma X$ cut, [Fig. 1(c)], we observe similar bands around $\theta = 0°$, while the spectral feature at $\theta$ larger than 10° looks significantly different from that in the $\Gamma K$ cut. To see more clearly the dispersive feature of bands, we have mapped out the band structure and show the result in Figs. 1(d) and 1(e) for the $\Gamma K$ and $\Gamma X$ directions, respectively. The experimental band structure is obtained by plotting the intensity of second derivatives of the spectral intensity as a function of wave vector and binding energy. Bright areas correspond to the experimental bands. We also show in Fig. 1(d) the band structure calculated with the empirical pseudopotential method along the $\Gamma K$ direction at $k_z = 0$ and $\pi$ (solid and broken lines, respectively) [16]. As clearly seen in Fig. 1(d), the experimentally determined valence-band structure shows a good agreement with the calculations for both $k_z = 0(\Gamma KX)$ and $\pi(XK\Gamma)$, indicating that bands with different $k_z$ values are simultaneously observed in the experiment due to the large $k_z$ broadening. Hence the obtained ARPES data mainly reflect the electronic states integrated over the $\Gamma X\Gamma X$ emission plane [red area in Fig. 1(a)], consistent with the previous ARPES reports on PbTe [17,18]. According to the band calculation, these bands are assigned to the Te $5p$ orbital with small admixture from the Pb $6p$ orbital. It is also inferred that the ARPES data along the $\Gamma X$ direction would reflect the electronic states integrated over the $\Gamma XXX$ emission plane [green area in Fig. 1(a)], although the band calculation at $k_z = \pi$ ($XWX$ direction) is not available [16]. It is noted here that quite similar valence-band dispersions are observed in the Tl-doped sample.

To clarify the change in the electronic structure upon Tl doping, we have performed angle-integrated PES measurement for pristine and Tl-doped PbTe ($x = 0.5$ at.%) and compare the result in Fig. 2. As clearly seen in Fig. 2, the angle-integrated PES spectrum which roughly reflects the valence-band DOS looks very similar between two samples, while the spectrum of the Tl-doped sample is slightly shifted as a whole toward low-binding energy by about 50 meV with respect to that of pristine sample. This demonstrates that 0.5% Tl doping causes a chemical potential shift of about 50 meV. This is further confirmed by the Pb $5d$ core-level PES measurement shown in the inset, where the spin-orbit-splitted Pb $5d_{3/2}$ and $5d_{5/2}$ peaks are shifted as a whole toward low binding energy by 50 meV upon Tl doping.

To see more clearly the change in the near-$E_F$ band structure upon Tl doping, we have performed high-resolution ARPES measurements along the cut around $\bar{X}$ point in the surface BZ [a green line shown in the inset to Fig. 3(a)]. The $\bar{X}$ point corresponds to the projection of the $L$ point in the bulk BZ where the band approaches closest to $E_F$. Figure 3 shows ARPES spectra measured at 20 K for

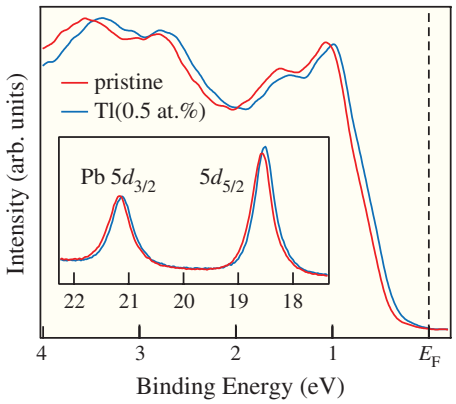


FIG. 2 (color). Angle-integrated PES spectra in the valence-band region of pristine (red line) and Tl0.5% (blue line) PbTe, measured with the He I$\alpha$ line. Inset shows the Pb $5d$ core-level PES spectra for each sample measured with the He II$\alpha$ line.

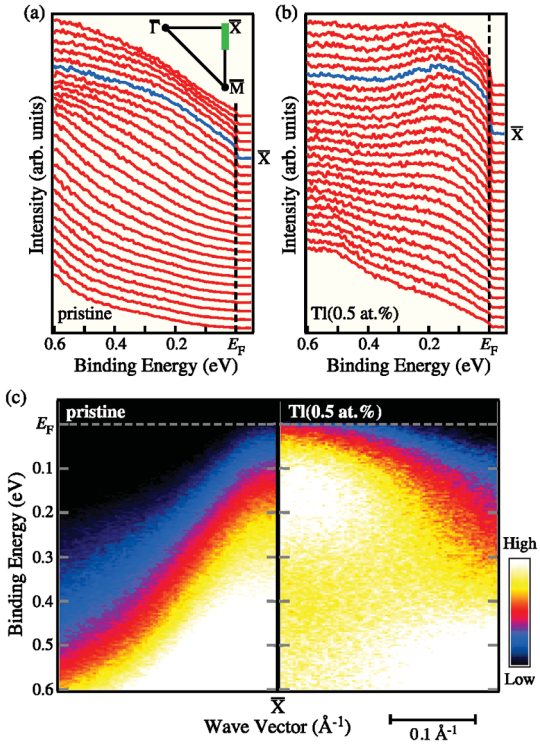


FIG. 3 (color). ARPES spectra near $E_F$ for (a) pristine and (b) Tl0.5% PbTe measured at 20 K with the He I$\alpha$ line along a green line in the surface BZ (inset). (c) ARPES intensity plots of (a) and (b) as a function of binding energy and wave vector.

(a) pristine and (b) Tl0.5% samples, together with (c) their intensity plots. It is expected from the band calculation [16] that when holes are doped into the valence band, a small FS will appear at first at the $L$ point of bulk BZ. We find in Fig. 3(a) a relatively broad dispersive feature in the pristine sample, which has the top of dispersion around the $\bar{X}$ point at about 0.2 eV. By comparing with the calculation [16], this dispersive band is assigned to the heavy hole band which has the top of dispersion halfway between the $\Gamma$ and $K$ points. We also find a broad shoulderlike feature in the low-binding-energy side toward $E_F$ [Fig. 3(a) and 3(c)], which is assigned to the calculated light hole band [16] having the top of dispersion at the $L$ point [19]. We infer that a small Fermi-edge structure in the ARPES spectra around the $\bar{X}$ point of the pristine sample may be explained in terms of a tiny hole doping due to Pb defects in the crystal [20]. In the Tl0.5% sample [Fig. 3(b)], the peak in the ARPES spectrum at the $\bar{X}$ point is shifted toward $E_F$ by approximately 50 meV, consistent with the result in Fig. 2. Furthermore, the spectral intensity at $E_F$ drastically increases and the momentum ($k$) region where a clear Fermi edge is seen is substantially expanded in comparison with that of a pristine sample. In contrast, no clear signature for the impurity level (band) at $E_F$ is seen because the Fermi-edge structure is observed in a relatively narrow $k$ region around the $\bar{X}$ point [Fig. 3(c)] contrary to the $k$-independent nature of localized impurity states. The absence of the localized states in the ARPES spectrum would not be ascribed to extrinsic reasons such as the spectral broadening due to the finite resolution and the small cross section of electrons in the Tl orbital, because the expected bandwidth of the localized states is comparable to the energy resolution of the present ARPES experiment [21], and the localized states should be resolved in the $k$ region where the valence-band intensity vanishes at $E_F$ even when the cross section of Tl electrons is relatively small. All these experimental results indicate that the substitution of Tl for Pb causes the direct hole doping into the light hole band of pristine PbTe. It is also noticed here that the ARPES spectrum of the Tl0.5% sample in Fig. 3 is not simply explained by a rigid-band model because the spectral line shape itself changes with doping. This change might be due to the binding-energy dependence of the lifetime of electrons near $E_F$ and/or a matrix-element effect in the photoexcitation process.

To elucidate the effect of Tl doping on the $k$ dependence of near-$E_F$ electronic states, we have performed high-resolution ARPES measurements to cover the full BZ. Figure 4 shows plots of the ARPES spectral intensity at $E_F$ measured at 20 K as a function of the two-dimensional wave vector in the surface BZ, for (a) pristine and (b) Tl0.5% samples. The spectral intensity was normalized to the integrated spectral intensity in the energy range of 0–4.8 eV which covers the whole valence-band region. In the pristine sample [Fig. 4(a)], we observe the finite intensity in a very small $k$ region centered at the $\bar{X}$ point, which corresponds to the Fermi edge originating in the light hole band [see Fig. 3(a)]. Upon Tl doping [Fig. 4(b)], this feature becomes large and intense, and evolves into a large spherelike FS. These changes with doping are robust to the normalization procedure, since the change in the electron number by Tl0.5% doping is negligible with respect to the total number of valence electrons. We confirmed this point by performing several normalizations with different energy

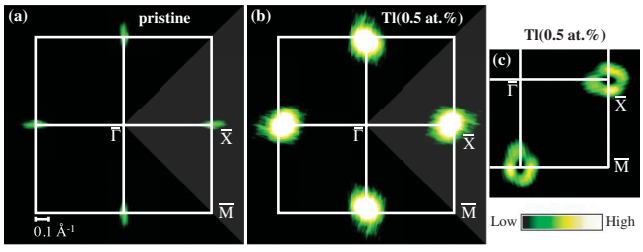


FIG. 4 (color). ARPES spectral intensity plots at $E_F$ as a function of the two-dimensional wave vector measured at 20 K with the He I$\alpha$ line for (a) pristine and (b) Tl0.5% samples. Spectral weight is integrated within 15 meV with respect to $E_F$. We have symmetrized the spectral weight by assuming the fourfold symmetry. A momentum region where the ARPES spectra were actually measured is shown by the gray triangle area. (c) Intensity plot of $|\mathrm{grad}_{\mathbf{k}}\, n(\mathbf{k})|$ for the Tl0.5% sample.

ranges. The topology of FS in Figs. 4(a) and 4(b) is hole-like judging from the band dispersion in Fig. 3, consistent with the positive value of the Hall coefficient [22]. We have roughly estimated the volume of FS of Tl0.5% PbTe as follows. We at first determined the position of Fermi vectors ($k_F$) in the surface BZ by tracing the local maxima of $|\mathrm{grad}_{\mathbf{k}}\, n(\mathbf{k})|$ [23] shown in Fig. 4(c). We assumed an ellipsoidal FS centered at the $L$ point elongated along the $\Gamma L$ direction as in the band calculation [16]. The estimated separation between two $k_F$ points along the $\bar{\Gamma}\bar{X}$ direction ($0.25 \pm 0.06$ Å$^{-1}$) is $1/\sqrt{2}$ of the longer axis ($2b$), while that along the $\bar{X}\bar{M}$ direction ($0.16 \pm 0.04$ Å$^{-1}$) is the same as the shorter axis ($2a$). The estimated volume of FS ($4\pi a^2 b/3$) with respect to the full BZ volume is $(5.1 \pm 2.8) \times 10^{-3}$, corresponding to the carrier concentration of $(1.5 \pm 0.8) \times 10^{20}$ cm$^{-3}$. This value is roughly consistent with the estimated value from the Hall coefficient ($\sim 0.6 \times 10^{20}$ cm$^{-3}$) [6]. The difference by a factor of 2–3 may be due to the finite resolution in the ARPES experiment which is likely to cause the overestimation of the FS volume and/or additional hole doping caused by Pb defects.

Now we discuss the implication of our experimental results in comparison with theoretical models. We summarize the present ARPES results: (i) Tl doping produces a shift of the valence band and the core level, (ii) nondispersive localized impurity states (bands) near $E_F$ are not clearly observed in the Tl0.5% sample, and (iii) the FS is observed only at the $\bar{X}$ point where the valence band of pristine PbTe is closest to $E_F$. All these experimental results suggest that the Tl doping of up to 0.5 at.% causes a direct hole doping into the valence-band top of pristine PbTe, but does not produce impurity states at $E_F$. Since the Tl concentration of the present sample ($x = 0.5$ at.%) exceeds the critical value ($x_c = 0.3$ at.%) where the hole concentration starts to saturate, we should have observed the quasilocalized impurity states at $E_F$, if the impurity states play an essential role for the saturation of the hole concentration. The present ARPES results suggest the electronic states of the Tl0.5% sample may not be well explained by the localized impurity-state model. On the other hand, the negative-$U$ model assumes that all Tl impurities in the compound act as $Tl^+$ for $x < x_c$ [13,15]. In this case, holes are doped into the valence band of PbTe, consistent with the chemical potential shift observed in the present experimental result. While the negative-$U$ model predicts a presence of the Kondo resonance peak near $E_F$ below the Kondo temperature ($T_K$) [13,15], we do not find a clear evidence for it in the ARPES spectrum, probably due to the relatively high temperature of ARPES measurements (20 K) compared to $T_K$ ($\sim$6 K). This point should be clarified in the future by ARPES measurements below $T_K$. The present ARPES result puts a constraint on the theoretical model to describe the electronic states of Tl-doped PbTe.

In conclusion, we found by ARPES that Tl doping in PbTe causes the direct hole doping into the top of valence band of pristine PbTe. We also found no clear evidence for the existence of the localized impurity states at $E_F$. These results suggest that the doped holes in the valence band of PbTe are responsible for the metallic conductivity in Tl-doped PbTe.

This work was supported by grants from JST-CREST and MEXT of Japan. K. N. thanks JSPS for financial support.

[1] J. Bardeen, L. Cooper, and J. R. Schrieffer, Phys. Rev. **108**, 1175 (1957).
[2] *The Physics of Superconductors*, edited by K. H. Bennemann, J. B. Bennemann, and J. B. Ketterson (Springer, New York, 2003).
[3] J. Merino and R. H. McKenzie, Phys. Rev. Lett. **87**, 237002 (2001).
[4] I. A. Chernik and S. N. Lykov, Sov. Phys. Solid State **23**, 817 (1981).
[5] V. I. Kaidanov and Y. I. Ravich, Sov. Phys. Usp. **28**, 31 (1985).
[6] Y. Matsushita, P. A. Wianecki, A. T. Sommer, T. H. Geballe, and I. R. Fisher, Phys. Rev. B **74**, 134512 (2006).
[7] H. Murakami *et al.*, Physica C (Amsterdam) **269**, 83 (1996).
[8] S. A. Nemov and Y. I. Ravich, Phys. Usp. **41**, 735 (1998).
[9] S. Ahmad, K. Hoang, and S. D. Mahanti, Phys. Rev. Lett. **96**, 056403 (2006).
[10] B. Y. Moizhes and I. A. Drabkin, Sov. Phys. Solid State **25**, 1139 (1983).
[11] H. B. Schuttler, M. Jarrell, and D. J. Scalapino, Phys. Rev. B **39**, 6501 (1989).
[12] M. V. Krasin'kov and B. Y. Moizhes, Sov. Phys. Solid State **33**, 202 (1991).
[13] M. Dzero and J. Schmalian, Phys. Rev. Lett. **94**, 157003 (2005).
[14] Y. Matsushita, H. Bluhm, T. H. Geballe, and I. R. Fisher, Phys. Rev. Lett. **94**, 157002 (2005).
[15] A. Taraphder and P. Coleman, Phys. Rev. Lett. **66**, 2814 (1991).
[16] G. Martinez, M. Schlüter, and M. L. Cohen, Phys. Rev. B **11**, 651 (1975).
[17] T. Grandke, L. Ley, and M. Cardona, Phys. Rev. B **18**, 3847 (1978).
[18] V. Hinkel *et al.*, Phys. Rev. B **40**, 5549 (1989).
[19] We have confirmed this point by mapping the three-dimensional band structure using the synchrotron radiation.
[20] R. Dornhaus *et al.*, *Narrow-Gap Semiconductors*, Springer Tracts in Modern Physics Vol. 98 (Springer-Verlag, New York, 1983).
[21] H. Murakami *et al.*, Physica C (Amsterdam) **273**, 41 (1996).
[22] I. A. Chernik, S. N. Lykov, and N. I. Grechko, Sov. Phys. Solid State **24**, 1661 (1983).
[23] T. Straub *et al.*, Phys. Rev. B **55**, 13 473 (1997).